Applied Surface Science 258 (2012) 7395–7400

Contents lists available at SciVerse ScienceDirect

Applied Surface Science

journal homepage: www.elsevier.com/locate/apsusc

Raman and TEM characterization of high fluence C implanted nanometric Si on insulator

R.M.S. dos Reis[a], R.L. Maltez[a,*], E.C. Moreira[b], Y.P. Dias[b], H. Boudinov[a]

[a] Instituto de Física, UFRGS, C.P. 15051, 91501-970, Porto Alegre, RS, Brazil
[b] Universidade Federal do Pampa – UNIPAMPA, Campus Bagé, 96400-970, Bagé, RS, Brazil

ARTICLE INFO

Article history:
Received 9 November 2011
Received in revised form 24 February 2012
Accepted 7 April 2012
Available online 12 April 2012

PACS:
68.55.ag
85.40.Ry
78.30.Hv
68.37.Lp
61.37.Og

Keywords:
C implantation
SiC layer on insulator
Ion beam synthesis
Raman spectroscopy
TEM

ABSTRACT

In this work we present Raman and transmission electron microscopy (TEM) characterization of high fluence C implanted nanometric silicon on insulator. The analyzed samples were 35 and 60 nm top layers of Si, which were entirely converted into SiC layers by 2.3×10^{17} cm^{-2} and 4.0×10^{17} cm^{-2} carbon implantations. We report the behavior of C—C signal from Raman spectra for such overall Si to SiC conversions before and after 1250 °C annealing. A remarkable effect is observed in the region of C signal (1100–1700 cm^{-1}), where fitting with Lorentzian curves reveals that there are different types of C—C bonds. Raman spectroscopy in this region was then employed to relatively characterize the SiC structural quality. TEM measurements support our Raman interpretation by direct structural evaluation of the formed SiC layers.

1. Introduction

Silicon carbide (SiC) is a promising semiconductor for high-power and high-frequency electronic devices [1]. SiC is also appropriate to work in reactive environments due to the strong bonding between Si and C. In addition, its large band gap (2.2–3.3 eV) is suitable for light emission in the green to blue range [1–3]. However, the light emitting recombination efficiency for SiC is only about 0.02% (indirect band gap), which can be partially compensated by the capability to work at higher current levels [4]. A disadvantage of SiC, however, is the high cost to grow large area wafers. Conversion of a thin surface layer of low cost Si wafers into SiC could be a possible solution for this issue. It has been shown [5–12] that ion beam synthesis (IBS) is an attractive method to obtain 3C—SiC layers on Si. SiC has also been used as buffer layer for further growth of other well-matched materials like GaN, ZnO and graphite layers [10,13–15]. Thus, such conversion would also be an alternative route to integrate these materials into the well-developed Si-base technology, once SiC is obtained on the top of silicon.

In previous works [6,7] we investigated the possibility of using carbon ion implantation to convert the nanometric Si overlayer of SIMOX (1 1 1) (Separation by IMplantation of Oxygen) into SiC layer. The real influence of the large lattice mismatch between Si and SiC on the crystalline quality of the synthesized SiC layer was evaluated since the existence of the buried oxide (BOX) in the SIMOX structure act as a buffer layer. This buffer layer allows stress relaxation between Si substrate and the synthesized SiC. The results [6] indicated that excess of C is the major detrimental factor to determine the final crystalline quality.

In this work, Raman spectroscopy was applied as a tool to observe the formation of C—C bonds in the synthesized SiC, as a function of the implanted C fluence, and to relatively characterize the structural quality among the formed structures. Raman was widely employed to characterize almost all carbonaceous materials [16–23]. The behaviors before and after high temperature annealing were also studied in order to discuss the modifications related to the thermal treatment. Raman technique is capable of differentiate signals of crystalline carbon regions from highly disordered ones and it is also sensitive to the C hybridization. Transmission electron

* Corresponding author. Tel.: +55 51 33086541; fax: +55 51 33087286.
E-mail address: maltez@if.ufrgs.br (R.L. Maltez).

0169-4332/$ – see front matter © 2012 Elsevier B.V. All rights reserved.
http://dx.doi.org/10.1016/j.apsusc.2012.04.044

microscopy (TEM) analysis was also employed to characterize the synthesized structures, presenting a direct observation of the SiC crystalline quality differences.

2. Experimental

SIMOX structures on a Si(1 1 1) bulk, with two different 1 1 1-silicon overlayer (SOV) thicknesses, were used as starting material for the synthesis: one with 65 nm of SOV (SIMOX65) and another with 35 nm of SOV (SIMOX35), both samples with 65 nm buried silicon dioxide layer (BOX). A 100 nm SiO_2 cap was deposited by CVD technique before implantation with C ions at 40 keV, with samples held at 600 °C, up to fluences of 2.3×10^{17} cm^{-2} (named low fluence) and 4.0×10^{17} cm^{-2} (named high fluence). The carbon fluences were chosen based on previously published studies [6,7], where it can be found more details about such SiC synthesis. The purpose of SiO_2 cap was to locate the implanted carbon peak close to the top SiO_2/SOV interface, aiming a complete conversion of the overlayer. The carbon depth distribution simulated by SRIM 2008 program [24] is a Gaussian like profile with a projected range of about 110 nm and a FWHM of about 78 nm. The SiO_2 cap of all implanted samples was removed by HF etching after C implantation and then annealed at 1250 °C in Argon (with 1% O_2) for 2 h. After final annealing, the samples were submitted to a new HF etching to remove any residual SiO_2. Raman spectra were obtained at room temperature by using a micro-positioning system B&WTek and an Andor Shamrock 303i monochromator. A thermo-electrically charge-cooled back illuminated deep depletion device was used for signal detection, enabling negligible dark current. A microscope equipped with a ×20 objective lens was used to focus the 532 nm excitation laser beam on the sample and to collect the Raman signal in the backscattered direction. The excitation power was kept at 0.20 mW/μm^2 in order to avoid any thermal effects. Transmission electron microscopy technique was employed, using the JEOL JEM 2010 transmission electron microscope of the Center for Electron Microscopy – UFRGS, operated at 200 kV of acceleration voltage.

3. Results and discussions

Fig. 1 presents typical Raman spectra (continuous line) obtained from a SIMOX sample as sketched on figure insert. Such spectrum from non-implanted sample (continuous line) shows a set of well-defined peaks corresponding to crystalline Si structure: the intense 520 cm^{-1} and two weaker peaks (270 cm^{-1} and 970 cm^{-1}). An important modification in the spectrum is observed comparing non-implanted sample with a C implanted one (full circles). A band arises in the region between 1100 and 1700 cm^{-1} due to the presence of carbon. This effect is connected to the formation of C compounds with different types of arrangements/bonds [16]. The nature of C—C bonds can be identified from a more detailed analysis of the Raman signal, as follows.

Raman spectroscopy conducted in the visible range provides information on the sp^2 constituents of amorphous carbon films. The Raman spectra of carbonaceous materials show two quite strong vibration modes, the G peak around 1580 cm^{-1} and the D peak around 1350 cm^{-1}, both features of the sp^2 bonds [16]. The G mode at 1580 cm^{-1} involves the in-plane bond-stretching motion of pairs of C sp^2 atoms. This mode does not require the presence of six-fold rings, and so it occurs at all sp^2 sites, not only those ones in rings [20]. The D peak around 1350 cm^{-1} is a breathing mode of the aromatic rings (collective identical movement of all six C atoms of the ring in radial direction). This mode is forbidden in perfect graphite and only becomes active in the presence of disorder in the graphite or non-compacted aromatic rings.

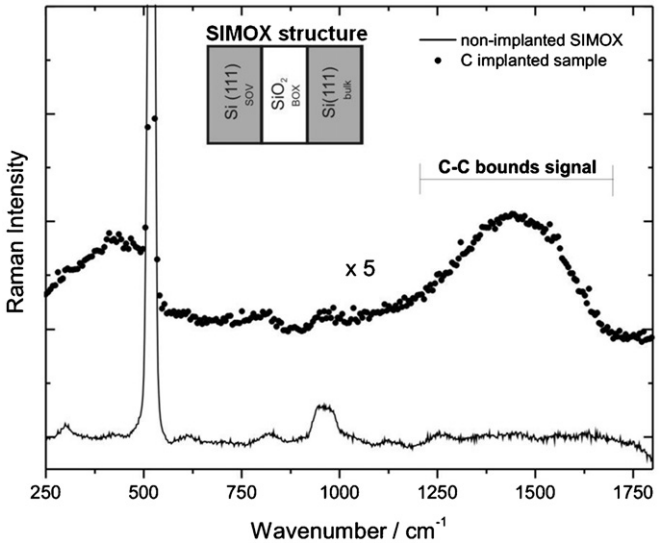

Fig. 1. Full range typical Raman spectra. Typical Raman spectra from a non-implanted SIMOX samples (continuous line) in comparison with an as-implanted high fluence SIMOX sample (full circles) one. Data was increased by 5× in order to demonstrate the main Raman spectra modifications due to C implantation. A SIMOX structure sketch is shown as insert.

We have also observed a weak signal around 800 cm^{-2} from Si—C bonds [25] (not shown here). However, such a low intensity Si—C signal for our samples, as compared to the one reported from a bulk SiC [25], is because we have synthesized a very narrow SiC layer (about 40 nm).

In Fig. 2 are presented Raman spectra acquired from high fluence implanted SIMOX samples with SOV of 65 nm (SIMOX65) before (Fig. 2(a)) and after (Fig. 2(b)) annealing in the region where the C effects are more remarkable (1100–1700 cm^{-1}). The experimental data (full circles) are fitted by a set of Lorentzian functions (continuous lines) to provide information about the origins of C—C bonds signals and their relative contributions. Two main contributions for C—C vibrational modes are the previously mentioned D and G peaks.

The annealing effect on this sample is clearly seen on Fig. 2(b) where both main contributions (D and G peaks) become better resolved. After the annealing the D peak appears at its standard position (1350 cm^{-1}), as observed on the literature [16]. It could be related to redistribution [7] and a better ordering of the carbon in the SiC layer, after annealing of the implanted sample, thus defining a better arrangement of C bonds.

Second order peaks were also inserted to obtain a better match of experimental data. Additional peak in the as-implanted Raman spectrum [Fig. 2(a)], around 1250 cm^{-1}, has been associated with mixed sp^2—sp^3 bonds [22]. A peak centered at 1608 cm^{-1} arises in the annealed case [Fig. 2(b)]. It is called D2 band and has been attributed to a lattice vibration analogous to that of the G band but, involving graphite termination planes [23], in our case, surrounded by crystalline SiC.

Fig. 3 shows Raman spectrum for a low fluence SIMOX65 sample after annealing (as-implanted spectrum for this case shows very weak C—C signal – not shown). Comparing Fig. 3 to Fig. 2(b) (high fluence sample), we observe that D2 band contribution drops in the low fluence sample. As previously mentioned, D2 band can be attributed to the occurrence of "isolated" graphite layers. In this sense, D2 drop indicates less graphite layers formed in between synthesized SiC material. Since the synthesized SiC crystal should not have any graphite layers in its structure, at our understanding, the D2 peak intensity decreasing indicates a better crystalline quality of the low fluence SIMOX65. This interpretation is corroborated

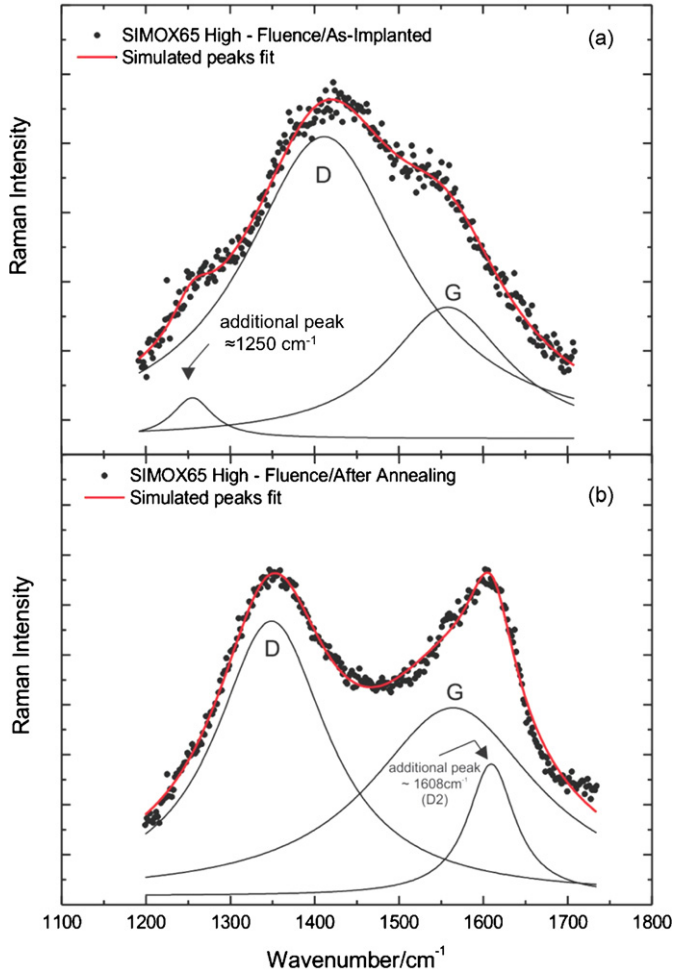

Fig. 2. High fluence implanted SIMOX65 Raman spectra. Raman spectra in a region between 1100 and 1800 cm^{-1} taken from High fluence implanted SIMOX65 in (a) as-implanted and (b) post-annealing cases. Lorentzian fit curves to each Raman signal are showed and a cumulative fit of them (continuous line) are superimposed to the experimental data (full circles).

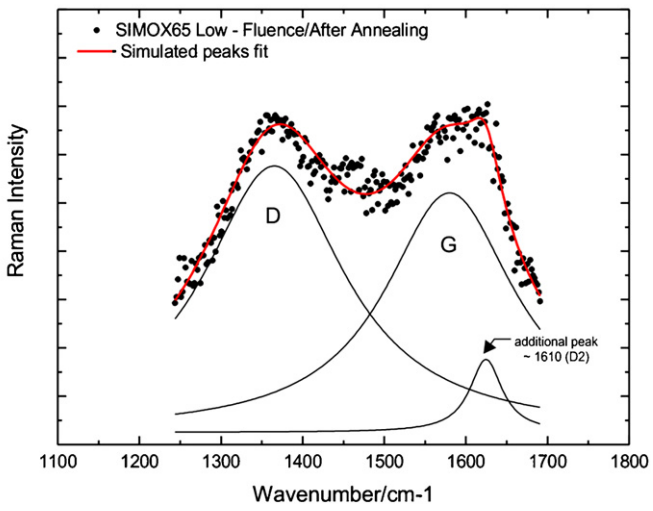

Fig. 3. Low fluence implanted SIMOX65 Raman spectrum. Raman spectrum in a region between 1100 and 1800 cm^{-1} taken from (a) low fluence SIMOX65 in after annealing. Lorentzian fit peaks to each Raman signal are showed with its cumulative curve fit (continuous line) superimposed to the experimental data (full circles).

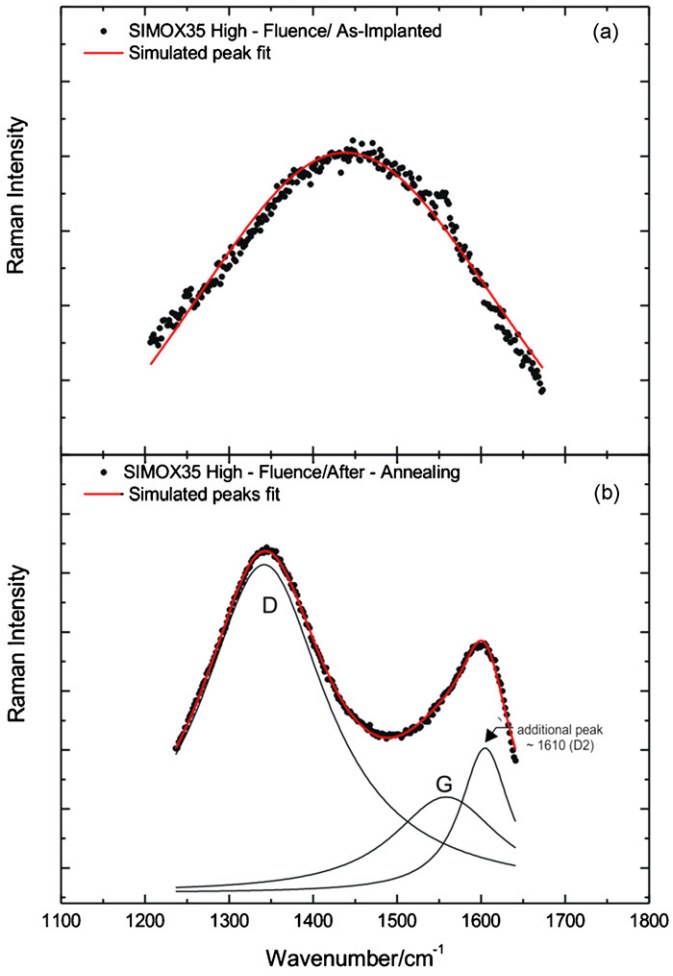

Fig. 4. High fluence implanted SIMOX35 Raman spectra. Raman spectra in a region between 1100 and 1800 cm^{-1} from high fluence implanted SIMOX35 in (a) as-implanted and (b) post-annealing cases. Lorentzian peaks and a cumulative curve fit (continuous line) are showed.

by TEM analysis (Fig. 5 – to be discussed later), which demonstrates a better crystal quality for the low fluence case.

To investigate the effect of excess of C, SIMOX samples with SOV of 35 nm (about half thickness of earlier samples) were C implanted with high fluence ($\Phi = 4.0 \times 10^{17}$ cm^{-2}) and submitted to the same thermal treatment. An important issue is that, in this case, the samples are over implanted, i.e. the C amount implanted is much more than the one necessary for the formation of a stoichiometric SiC layer [6,7]. Thus, there will be more C atoms available to form C—C bonds. Fig. 4(a) shows Raman spectra from as-implanted and Fig. 4(b) from annealed cases for this sample. Fig. 4(a) shows a broad continuous band in the as-implanted case, probably associated with mix-up of C—C bonds. Fig. 4(b) shows the split in two well defined peaks after annealing, as in the case of high fluence SIMOX65 sample, that we have attributed to redistribution and better ordering of the carbon in the SiC layer. The fitting spectrum from Lorentzian functions shows contributions of D, G and D2 peaks. As will be shown later, in the TEM analysis of Fig. 5(c), this sample is the most disordered one (almost an amorphous SiC, with high excess of C atoms) containing randomly oriented cubic SiC grains. Then, the relative increase of D2 peak intensity indicates a higher SiC crystal quality degradation.

It has been observed [16–19], that the ratio of the D and G peak intensities, $R = I_D/I_G$, is inversely proportional to the effective crystalline size in polycrystalline graphite. In a more extensive

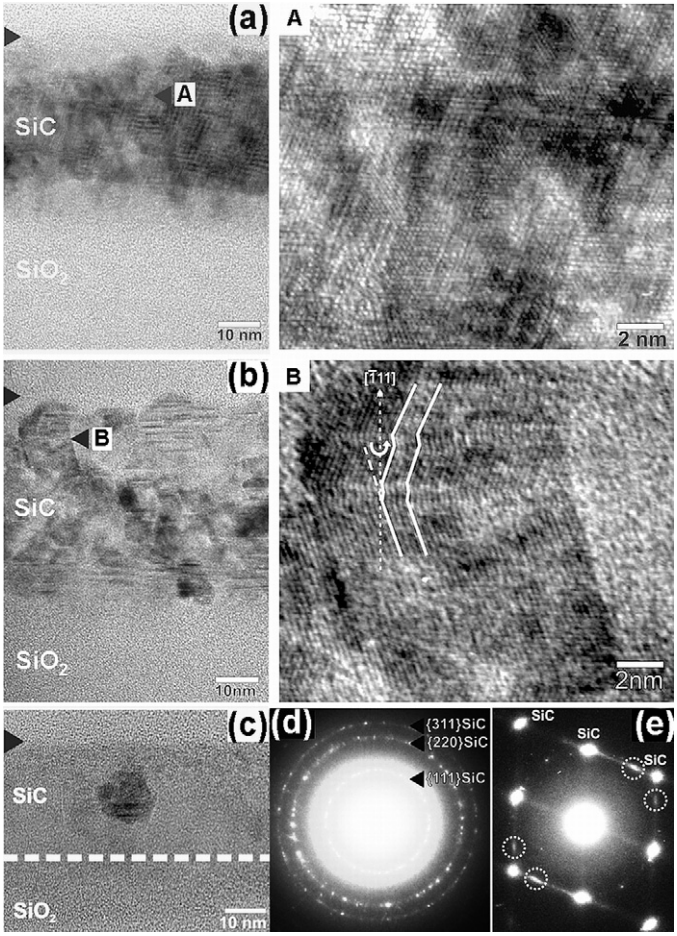

Fig. 5. Cross-sectional HRTEM micrographs and SAD patterns. (a)–(c) Cross-sectional HRTEM micrographs, taken along [1 1 0] zone axis, of annealed samples (sample surface marked by the arrowhead at the left-hand side): (a) low fluence SIMOX65 (right side is magnified view of area marked with the arrowhead A), (b) high fluence SIMOX65 (right side is magnified view of area marked with the arrowhead B) and (c) high fluence SIMOX35. (d) and (e) SAD patterns taken exclusively from synthesized SiC layers showed in images (c), and (b), respectively.

interpretation we could claim that a decrease of R-value indicates an increase of the crystal quality of the C structures. Then, this interpretation could be extended to other carbonaceous materials. An important issue is that we are not analyzing graphitic samples but SiC ones, and it is not clear that we can extrapolate a similar interpretation to our case. However, if we do so, we can see a systematic increase of the R-value for the annealed samples on the following sample sequence: low fluence SIMOX65 ($R = 1.1$), high fluence SIMOX65 ($R = 1.3$, i.e. 18% increase), high fluence SIMOX35 ($R = 2.3$, i.e. 110% increase). This increase might be interpreted as a consequence of a decrease of well-ordered areas in the formed SiC layer, in the sense of obtain a better quality of C structures as a result of a good SiC layer quality around these ones. We will show later that these results are in total agreement with the TEM analysis.

In addition, we also evaluated an additional parameter aiming to explain the Raman results and to relate it directly with a SiC crystal quality. A new R_C parameter was defined as the ratio of the spectrum area in the wavenumber range from 1100 up to 1700 cm^{-1} (where the peaks D, D2 and G can be found, all related to C bonds contributions to the Raman spectra) by the area under the peak corresponding to the bulk crystalline Si substrate structure (520 cm^{-1} – see Fig. 1).

To obtain such evaluation, we used the net area in the wavenumber range from 1100 up to 1700 cm^{-1} where background signal is subtracted from the raw data. At this point is good to notice that the C Raman signal comes from 30 to 50 nm thick synthesized SiC layers, which are on the sample surface. Thus, the Raman Si signal from the Si substrate can be considered constant, since the penetration depth of the excitation wavelength (about 700 nm in Si) is much larger than the width of the nanometric SiC layer on its surface (or its variation). This is why such a ratio R_C defined in relation to the Si substrate peak intensity (which would have about the same intensity if all analyzed samples are submitted to an equivalent laser pumping condition), normalizes the C bonds contribution and allows a direct comparison among distinct samples.

The observed sequence for the R_C parameter (0.14, 0.58, and 1.35, respectively) agrees with R parameter behavior. Both results, for R and R_C parameters, are summarized in Table 1 where we also show the Lorentzian fittings for all samples, showing the wavenumber value and the FWHM of each peak. We notice that the R_C parameter appears to be more sensitive to changes in the crystal quality: it shows 315% and 870% increases for the annealed samples high fluence SIMOX65 and high fluence SIMOX35, respectively, in relation to the value of the annealed low fluence SIMOX65. The high sensitivity of the R_C parameter, in addition to its simple interpretation as being proportional to the amount of C—C bonds formed in the SiC layer, where we should have just Si—C bonds in a perfect crystal, makes the R_C a good additional parameter to relatively probe the crystalline quality among nanometric SiC layers formed on Si substrates, when the Si—C direct signal is very weak or null in the spectra.

Additionally, R_C parameter could also be evaluated for as-implanted spectra, instead R parameter could not always be. See, for example, as-implanted spectra in Fig. 2(a) (high fluence SIMOX65) and Fig. 4(a) (high fluence SIMOX35) which show broad bands where D and G contributions are badly or even not resolved at all. The results for as-implanted samples show R_C parameters, which are lower than the corresponding ones obtained after annealing at 1250 °C. This is coherent with an important C redistribution [7] and better ordering of the C implanted atoms in the synthesized layer during annealing. This increase in R_C indicates that annealing promotes C dangling bonds passivation, either by forming C—C or C—Si bonds, depending on its local surroundings. However, at this point we would like to stress that R_C parameter is supposed to be applied just to compare SiC samples to each other and not for any type of alloys in which C—C bonds could be present in its perfect crystalline state.

In order to better understand the Raman results, Fig. 5(a–c) shows high resolution TEM (HRTEM) images from annealed samples: (a) low fluence SIMOX65, (b) high fluence SIMOX65 and (c) high fluence SIMOX35. The sample surface is at the top, indicated by the arrow at the left-hand side. The layers above the buried SiO_2 are the synthesized SiC ones after annealing, and they have thickness of about 40, 45 and 30 nm, respectively.

A comparison between TEM images Fig. 5(a and b), shows a better relative SiC crystalline quality for the SIMOX65 low fluence sample [Fig. 5(a)]. At their right side, we have placed a magnified view of the areas pointed with the arrowheads A and B inserted in Fig. 5(a and b), respectively. They confirm the better crystalline nature of the SiC layer formed in the low fluence sample [Fig. 5(a)] in respect to the high fluence one [Fig. 5(b)]. In particular for the later, the magnified view reveals crystalline regions which have a high density of twins on {1 1 1} planes (see the zig zag of the white lines in the figure).

TEM analysis shows that high fluence SIMOX65 sample [Fig. 5(b) and its zoom B] has higher structural damage as compared to the low fluence SIMOX65 one [Fig. 5(a) and its zoom A]. This is consistent with the observed increase in the parameters R and R_C of the high fluence and annealed SIMOX65 in comparison to the low fluence and annealed SIMOX65 (see Table 1). It is clear a

Table 1
RAMAN analysis summary. Wavenumber values and FWHM for D and G peaks and R and R_C ratios for each spectrum.

Sample	Peak	Wavenumber ($cm-^{-1}$)	FWHM (cm^{-1})	R (I_D/I_G)	R_C ($I_{Carbon}/I_{Silicon}$)
Low fluence SIMOX65 annealed	D	1365	211	1.1	0.14
	G	1579	193		
High fluence SIMOX65 As-implanted	D	1411	232	–	0.19
	G	1558	178		
High fluence SIMOX65 annealed	D	1348	160	1.3	0.58
	G	1565	240		
High fluence SIMOX35 As-implanted	D	1450 (single peak)	–	–	0.44
	G		–		
High fluence SIMOX35 annealed	D	1341	185	2.3	1.35
	G	1558	160		

grain nature present in the HRTEM image from the high fluence SIMOX65 sample [Fig. 5(b)], which is mainly due to the occurrence of highly disordered crystalline regions (like amorphous inclusions) in between grains of better ordered regions. We believe that in such highly disordered inclusions there is a higher density of C—C bonds in comparison to the better ordered grains of the low fluence SIMOX 65 sample [Fig. 5(a)]. In such highly disordered areas, one C atom may present up to 4 C—C bonds, depending on the local atomic environment and the hybridization condition. However, even in the better ordered regions of the high fluence SIMOX65, the observed high density of nanometric twins also justifies the existence of additional C—C bonds as a consequence of SiC "wrong bonds".

However, the structural degradation of the high fluence SIMOX35 sample [Fig. 5(c)] is much worst. The HRTEM image Fig. 5(c) and its corresponding selected area electron diffraction (SAD) [Fig. 5(d)], demonstrate a highly disordered layer. In special, the electron diffraction [Fig. 5(d)] is characterized by ring patterns, which demonstrates the existence of randomly oriented SiC cubic grains in the layer. Some large SiC grains [10 nm diameter] are eventually seen along the synthesized layer, as shown in the HRTEM image from the sample [Fig. 5(c)]. Such cross-section image [Fig. 5(c)] also demonstrates that the grains are found embedded in a very disordered SiC layer (almost an amorphous one). As a matter of fact, the R and R_C parameters for this sample are the highest one. Specially $R_C = 1.35$ for this sample (after annealing) that means, when compared to the low fluence SIMOX65 sample ($R_C = 0.14$ – the lowest damaged one), an increase by a factor of about 10 regarding C bonds, even though the implanted carbon amount was just increased by a factor of 1.8.

Finally, for comparison purpose, we show in Fig. 5(e) the SAD pattern from the high fluence SIMOX65 sample, whose image is in Fig. 5(b). In this SAD (as well in the previous one) there is no contribution from the Si substrate below the buried oxide layer [Si(1 1 1) substrate is even not shown in Fig. 5(a–c)]. Note that this SAD [Fig. 5(e)] indeed shows just spots characteristic of an synthesized cubic SiC structure and no spots from any residual crystalline Si unconverted region, which means a complete Si to SiC conversion. However, additional extra spots are present from twinned regions of SiC [the ones surrounded by doted circles in Fig. 5(e)]. Even though there is a high level damage in the high fluence SIMOX65 sample showed in Fig. 5(b), which is also evident by the presence of extra spots from twinned crystalline regions in its SAD [Fig. 5(e)], there is no doubt that the high fluence SIMOX35 [Fig. 5(c)] is the most degraded among all the samples, showing an almost amorphous and polycrystalline nature. Such structural analysis from TEM is completely coherent with the behavior presented by the R and R_C parameters and by the interpretation given for the D2 peak.

4. Conclusions

The shape and net intensity of the Raman spectra in the wave number range from 1100 to 1700 cm^{-1} show a strong dependence with the structural quality of nanometric SiC layer (30–45 nm thick) synthesized by C ion implantation into Si overlayer of SIMOX structures. We have studied changes in the shape mainly through R parameter, defined as the D to G peak intensities ratio, and found it is related to the quality of the synthesized SiC layers. R parameter interpretation in the SiC context is not clear because D and G signals are related to C—C bonds. Nevertheless, we have suggested that a better quality of C structures in the layer is a consequence of a good SiC layer quality around these ones, then indirectly probing the SiC layer quality. However, R parameter could not be evaluated for some as-implanted samples, either because there is a badly resolved D and G peaks or because just a single peak is observed (high damaged samples). To overcome these issues, the indirect SiC probing and non-resolved D and G peaks, we defined a new R_C parameter as the ratio between the net areas of the Raman signals in the 1100–1700 cm^{-1} region to the area of the Si substrate peak (520 cm^{-1}). This parameter is related to the intensity in Raman C—C region where the Si substrate signal just normalizes spectra to each other. Its interpretation is simpler and more directly related to the SiC structure: R_C parameter increases as SiC crystal quality decreases since a perfectly crystalline SiC layer must not have any C—C bonds, for which $R_C = 0$. The conclusion drawn through R_C parameter was the same that obtained through R parameter: low fluence SIMOX65, high fluence SIMOX65 and high fluence SIMOX35 are, in this order, the increased damage sequence. However, R_C parameter has a more clear interpretation in the SiC context and has showed higher sensitivity.

The structural quality was independently verified by TEM analysis, and it is in total agreement with the results obtained from Raman spectroscopy represented by R and R_C parameters.

Acknowledgments

The authors gratefully acknowledge financial support from FAPERGS, CNPq and Capes.

References

[1] H. Morkoç, S. Strite, G.B. Gao, M.E. Lin, B. Sverdlov, M. Burns, Large-band-gap SiC, III–V nitride, and II–VI ZnSe-based semiconductor device technologies, Journal of Applied Physics 76 (1994) 1363.
[2] Y. Matsushita, T. Nakata, T. Uetani, T. Yamaguchi, T. Niina, Fabrication of SiC blue LEDs using off-oriented substrates, Japanese Journal of Applied Physics 29 (1990) L343.
[3] M. Ikeda, T. Hayakawa, S. Yamagiwa, H. Matsunami, T. Tanaka, Fabrication of 6H—SiC light-emitting diodes by a rotation dipping technique: electroluminescence mechanisms, Journal of Applied Physics 50 (1979) 8215.
[4] J.A. Edmond, H.S. Kong, C.H. Carter Jr., Blue LEDs, UV photodiodes and high-temperature rectifiers in 6H—SiC, Physica B 185 (1993) 453.
[5] R.L. Maltez, R.M. de Oliveira, R.M.S. dos Reis, H. Boudinov, Ion beam synthesis of cubic-SiC layer on Si(1 1 1) substrate, Journal of Applied Physics 100 (2006) 063504.
[6] R.M.S. dos Reis, R.L. Maltez, H. Boudinov, Ion beam synthesis of SiC by C implantation into SIMOX(1 1 1), Nuclear Instruments and Methods in Physics Research B 267 (2009) 1281.
[7] R.M.S. dos Reis, R.L. Maltez, H. Boudinov, Carbon redistribution in nanometric $Si_{1-x}C_x$ layers upon ion beam synthesis of SiC by C implantation into SIMOX(1 1 1), Journal of Physics D: Applied Physics 43 (2010) 395401.

[8] P. Martin, B. Daudin, M. Dupuy, A. Ermolief, M. Olivier, A.M. Papon, G. Rollond, High-temperature ion beam synthesis of cubic SiC, Journal of Applied Physics 67 (1990) 2908.
[9] Y. Ito, T. Yamauchi, A. Yamamoto, M. Sasase, S. Nishio, K. Yasuda, Y. Ishigami, Ion beam synthesis of 3C—SiC layers in Si and its application in buffer layer for GaN epitaxial growth, Applied Surface Science 238 (2004) 159.
[10] A. Yamamoto, T. Yamauchi, T. Tanikawa, M. Sasase, B.K. Ghosh, A. Hashimoto, Y. Ito, Organometallic vapor phase epitaxial growth of GaN on a 3C—SiC/Si(1 1 1) template formed by C^+-ion implantation into Si(1 1 1) substrate, Journal of Crystal Growth 261 (2004) 266.
[11] J. Ristic, et al., Growth of GaN layers on SiC/Si(1 1 1) substrate by molecular beam epitaxy, Materials Science and Engineering B 93 (2002) 172.
[12] J.K.N. Lindner, Ion beam synthesis of buried SiC layers in silicon: basic physical processes, Nuclear Instruments and Methods in Physics Research B 178 (2001) 44.
[13] J. Komiyama, Y. Abe, S. Suzuki, H. Nakanishi, Stress reduction in epitaxial GaN films on Si using cubic SiC as intermediate layers, Journal of Applied Physics 100 (2006) 033519.
[14] A.J. van Bommel, J.E. Crombeen, A. van Tooren, LEED and Auger electron observations of the SiC(0 0 0 1) surface, Surface Science 48 (2) (1975) 463.
[15] Z.D. Sha, et al., Initial study on the structure and optical properties of ZnO film on Si(1 1 1) substrate with a SiC buffer layer, Physica E 33 (2006) 263.
[16] F. Tuinstra, J.L. Koenig, Raman spectrum of graphite, Journal of Chemical Physics 53 (1970) 1126.
[17] J.-N. Rouzaud, A. Oberlin, C. Beny-Bassez, Carbon films: structure and microtexture (optical and electron microscopy, Raman spectroscopy), Thin Solid Films 105 (1983) 75.
[18] P.D. Green, C.A. Johnson, K.M. Thomas, Applications of laser Raman microprobe spectroscopy to the characterization of coals and cokes, Fuel 62 (1983) 1013.
[19] A. Cuesta, P. Dhamelincourt, J. Laureyns, A. Martinez-Alonso, J.M.D. Tascon, Raman microprobe studies on carbon materials, Carbon 32 (1994) 1523.
[20] T. Jawhari, A. Roid, J. Casado, Raman spectroscopic characterization of some commercially available carbon black materials, Carbon 33 (1995) 1561.
[21] P. Lespade, A. Marchand, M. Couzi, F. Cruege, Caracterisation de materiaux carbones par microspectrometrie Raman, Carbon 22 (1984) 375.
[22] W.S. Bacsa, J.S. Lannin, D.L. Pappas, J.J. Cuomo, Raman scattering of laser-deposited amorphous carbon, Physical Review B 47 (1993) 10931.
[23] G. Katagiri, H. Ishida, A. Ishitani, Raman spectra of graphite edge planes, Carbon 26 (1988) 565.
[24] J.F. Ziegler, J.P. Biersack, U. Littmark, The Stopping and Range of Ions in Solids, vol. 1, Pergamon Press, Oxford, 1985.
[25] S. Nakashima, H. Harima, Raman investigation of SiC polytypes, Physica Status Solidi (a) 162 (1997) 39.